Available online at www.sciencedirect.com
SCIENCE DIRECT®
European Journal of Mechanics B/Fluids 23 (2004) 681–694

Stability of an ice sheet on an elastic bed

Alexander V. Wilchinsky [a,b,*], Daniel L. Feltham [a]

[a] *Centre for Polar Observation and Modelling, University College, London, UK*
[b] *Institute of Mathematics and Mechanics, Kazan State University, Russia*

Received 21 May 2003; received in revised form 10 August 2003; accepted 19 December 2003

Available online 7 February 2004

Abstract

The stability of stationary flow of a two-dimensional ice sheet is studied when the ice obeys a power flow law (Glen's flow law). The mass accumulation rate at the top is assumed to depend on elevation and span and the bed supporting the ice sheet consists of an elastic layer lying on a rigid surface. The normal perturbation of the free surface of the ice sheet is a singular eigenvalue problem. The singularity of the perturbation at the front of the ice sheet is considered using matched asymptotic expansions, and the eigenvalue problem is seen to reduce to that with fixed ice front. Numerical solution of the perturbation eigenvalue problem shows that the dependence of accumulation rate on elevation permits the existence of unstable solutions when the equilibrium line is higher than the bed at the ice divide. Alternatively, when the equilibrium line is lower than the bed, there are only stable solutions. Softening of the bed, expressed through a decrease of its elastic modulus, has a stabilising effect on the ice sheet.

Keywords: Ice sheet; Stability

1. Introduction

Many geophysical and environmental problems are described by slow spreading of a heavy fluid under the action of gravity [1–3]. The main features of these phenomena are that inertia is negligible and viscous forces balance the gravity-driven pressure gradient force; the aspect ratio of the heavy fluid is small; and the flow direction is close to horizontal [1]. The range of physical phenomena characterised by these features is broad, e.g., the flow of lava [2], lithosphere [4], ice sheets [5] and oil [6]. Here, we focus on ice sheet flow. Ice sheets flow as gravity currents with a non-Newtonian rheology, but are also characterised by regions of mass accumulation and ablation at their upper, free surface. Balance between accumulation upstream and ablation downstream allows the possibility of stationary-state solutions.

In the limit that the accumulation rate does not depend on the elevation, the bed is rigid, and the ice sheet front is fixed, it has been shown that a stationary solution is stable [7–9]. However, the mass accumulation on an ice sheet generally *does* depend on the upper surface elevation [10,11]. This reflects the dependence of weather conditions on elevation above sea level. Typically, in the upper part of an ice sheet, accumulation from snowfall is positive, whilst in the lower part accumulation is negative due to melting and ablation. These regions are separated by the so-called *equilibrium line* of zero accumulation. The dependence of the accumulation rate on elevation can lead to the instability of a stationary ice sheet to perturbations of its free surface. This is caused by the positive feedback between a local elevation of the free surface and the consequent increase of the mass-accumulation rate on it. Since the increase in accumulation causes the ice sheet to advance through an increase of the

* Corresponding author. CPOM, Dept. of Space and Climate Physics, UCL, Gower Street, London, WC1E 6BT, UK.
E-mail address: aw@cpom.ucl.ac.uk (A.V. Wilchinsky).

0997-7546/$ – see front matter
doi:10.1016/j.euromechflu.2003.12.004

horizontal mass flux, instability arises when the horizontal mass flux increase is insufficient to remove the extra accumulated mass. The principle of this instability was recently demonstrated for flow of Newtonian ice sheets over rigid bedrocks [12].

Motion of an ice sheet is also affected by glacial isostasy as the elastic lithosphere over which the ice sheet flows sinks under the weight of the ice sheet [13]. Sinking of the Earth's crust may diminish the free surface instability because an increase in accumulation yields a smaller rise of the free surface. The aim of this work is to study the influence of the bed form and its elasticity on the linear stability of a two-dimensional, and *non-Newtonian* ice sheet with elevation-dependent mass accumulation. This extends the previous study [12] by treating glacial isostasy and using Glen's flow law [14], which is a more realistic description of ice rheology and necessary for application to real ice sheets.

This paper is divided as follows: Section 2 presents the model, non-Newtonian Stokes flow and the scaling analysis appropriate for near stationary ice sheet flow. Section 3 presents the perturbation equations and addresses the singularity at the moving front using matched asymptotics. Some of this analysis is placed in the appendices. In Section 4, the eigenvalue problem determining stability is solved numerically for parameter combinations describing the role of bed slope, bed softness and equilibrium line inclination. This is followed by a discussion of results in Section 5, and our main conclusions are summarised in Section 6.

2. Physical model and stationary solutions

Here we consider two-dimensional isothermal Stokes flow of ice (Fig. 1). The density and viscosity of the ambient atmosphere will be neglected. We assume the slope of the bed to be comparable with that of the upper surface of the ice sheet, so that the longitudinal pressure drop caused by the free surface gradient and gravity force acting along the inclined bed are the main driving forces for the ice flow. These are balanced by the vertical gradient of the shear stress. The bed is assumed to be an elastic layer of constant (unloaded) thickness supported by a rigid surface, while the accumulation rate depends on the elevation of the top of the ice sheet. The ice rheology in creeping motion will be described by a power-law dependence of the effective viscosity on the second invariant of the strain-rate.

The following notation for the dimensional variables is used: $(\overline{X}, \bar{z})$ are the horizontal and upward vertical spatial coordinates, $\bar{t}$ is time, $\bar{u}$ and $\overline{w}$ are the ice sheet horizontal and vertical velocities, $\bar{p}$ is the pressure. The bed and free surface elevations are $\overline{B}$ and $\bar{s}$ respectively, $\overline{B}_0$ is the elevation of the unloaded bed, $\overline{H}_{(e)}$ is the constant thickness of the unloaded elastic layer, and $\bar{h} = \bar{s} - \overline{B}$ is the thickness of the ice sheet. The magnitude of gravitational acceleration is g, $\bar{A}$ is the accumulation rate at the free surface, which is assumed not to depend on time and not to decrease with $\bar{z}$, and ϱ is the ice density. The effective ice viscosity $\bar{\mu}$ in Glen's flow law is given by

$$\bar{\mu} = 2^{(1-n)/n} \eta^{1/n} II_{(d)}^{(1-n)/(n)}, \tag{1}$$

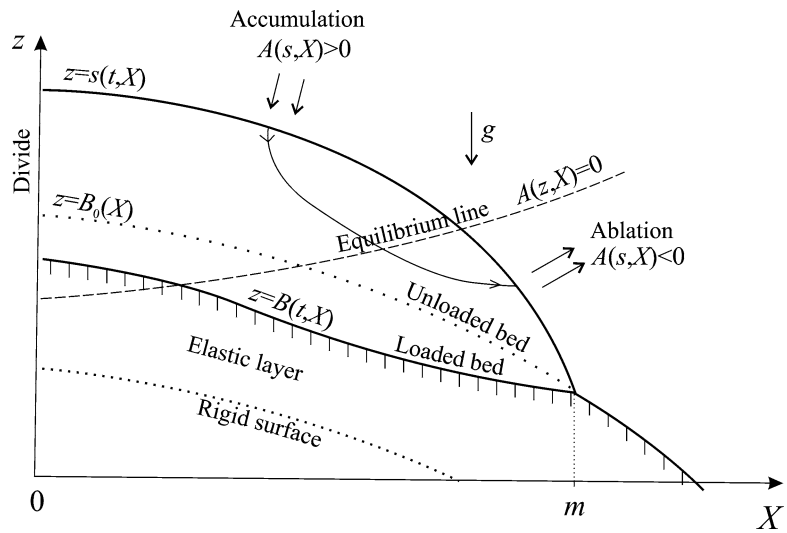

Fig. 1. An ice sheet on an elastic bed under the action of elevation-dependent surface mass-accumulation.

where η is the flow law constant, n is the flow law exponent in the power-law rheology of an incompressible fluid ($n \geqslant 1$ as ice is a pseudoplastic fluid), and $II_{(d)} = \{\frac{1}{2}[u_x^2 + w_z^2 + \frac{1}{2}(u_z + w_x)^2]\}^{1/2}$ is the second invariant of the strain-rate tensor. The stress tensor in the elastic lithosphere is given by the linear law [15]

$$\bar{\sigma}_{(ij)} = \frac{E}{1+\sigma}\left(\bar{e}_{(ij)} + \frac{\sigma}{1-2\sigma}\bar{e}_{(kk)}\delta_{(ij)}\right), \tag{2}$$

where $\bar{e}_{(ij)}$ is the strain in the elastic layer, σ, E are the Poisson's ratio and the Young's modulus of the elastic material. Letter subscripts without parentheses denote partial derivatives.

Typically, the lubrication approximation is used to simplify the Stokes equations describing ice sheet flow to derive the evolution equation for ice sheet thickness, e.g., [16,17,1]. Here, we consider the dynamics of the ice sheet near a stationary state determined by the accumulation-rate distribution. The scaling analysis is different to that for free spreading of a gravity current without accumulation and we briefly present this analysis.

Because the ice flow is determined by the mass accumulation and the no-slip condition is assumed at the bed, scales can be chosen as $[\overline{w}] = [\bar{A}]$, $[\bar{u}] = [\overline{w}]/\delta$, $[\bar{p}] = [\bar{z}]\varrho g$, $[\bar{t}] = [\bar{z}]/[\bar{A}]$, $\delta = [\bar{z}]/[\overline{X}] \ll 1$ (see discussion [8]). In dimensionless variables void of bars, the Stokes equations take the form

$$p_X = \varsigma\big[(\mu u_z)_z + \mathrm{O}\big(\delta^2\big)\big], \qquad p_z + \mathrm{O}\big(\varsigma\delta^2\big) = -1, \tag{3}$$

where

$$\mu = |u_z|^{(1-n)/n} + \mathrm{O}\big(\delta^2\big), \qquad \varsigma = \frac{(\eta[\bar{A}])^{1/n}[\overline{X}]^{(n+1)/n}}{\varrho g[\bar{z}]^{2(n+1)/n}}.$$

The stress-free condition at the top of the ice sheet (air drag is negligible) imply

$$\mu u_z = \mathrm{O}\big(\varsigma\delta^2\big), \qquad p = \mathrm{O}\big(\delta^2\big), \tag{4}$$

while mass conservation in a vertical column yields

$$h_t + q_X = A, \qquad q = \int_B^s u\,\mathrm{d}z, \tag{5}$$

where q is the horizontal mass flux. Scaling arguments applied to $(3)_1$ suggest that ς be of order unity. We let $\varsigma = 1$, which defines the relation between the horizontal and vertical scales $[\bar{z}]$, $[\overline{X}]$ [18]. The aspect ratio is then

$$\delta = \left(\frac{\eta[A]}{(\rho g)^n[\overline{X}]^{n+1}}\right)^{1/(2n+2)}. \tag{6}$$

Neglecting the terms of order $\mathrm{O}(\delta^2)$ and integrating $(3)_1$ and $(3)_2$ with respect to z, we obtain

$$p = s - z, \qquad u = \mathrm{sign}(s_X)|s_X|^n\big[(s-z)^{n+1} - h^{n+1}\big]/(n+1). \tag{7}$$

Substitution of $(7)_2$ for u into the mass conservation equation (5) yields the evolution equation for the thickness of the ice sheet

$$h_t + q_X = A(s, X), \qquad q = -\,\mathrm{sign}(s_X)h^{n+2}|s_X|^n/(n+2). \tag{8}$$

Similar scaling arguments can be applied to the equation for the vertical displacement in the underlying elastic layer, ζ, to give

$$\zeta_{zz} = \mathrm{O}\big(\delta^2\big), \tag{9}$$

which must satisfy the boundary condition at the supporting rigid surface, $\zeta = 0$ at $z = B_0 - H_{(e)}$, and stress continuity at the bottom of the ice sheet, $E(1-\sigma)(1+\sigma)^{-1}(1-2\sigma)^{-1}\zeta_z = \varrho g\bar{h} + \mathrm{O}(\delta)$. To $\mathrm{O}(\delta)$, the solution for the vertical displacement is

$$\zeta = kh\big[1 + (z - B_0)/H_{(e)}\big], \tag{10}$$

where $k = \varrho g(1+\sigma)(1-2\sigma)/[E(1-\sigma)\overline{H}_{(e)}]$ is a measure of the bed softness, and the displacement of the bed surface is $B_0 - B = kh$. The surface elevation of the ice sheet is thus

$$s = B_0 + (1-k)h. \tag{11}$$

Eq. (10) may be interpreted as a statement of hydrostatic equilibrium between the ice body and the bed upon which it rests, a frequently used assumption in ice sheet modelling (e.g., [19]), where k is the ratio of ice to bed density.

When accumulation rate depends only on elevation, then since $A_s \geqslant 0$, the length of a stationary ice sheet is finite only if the bed is higher than the equilibrium line $A(z, X) = 0$ within a finite region. In this case, the bed profile is convex with ice

spreading out from the divide, see Fig. 1. Because the mass flux at the divide is known, we study the ice motion from the divide to the flow front.

The non-linear parabolic equation (8) requires two boundary conditions and one initial condition for identification of its solution. If the ice spreads freely, then a third condition is necessary to determine the position of the flow front (margin), m. We use the fact that the horizontal mass flux is zero at the divide, and the thickness of the ice sheet and value of the horizontal mass flux at the front are also zero

$$q = 0 \quad \text{at } X = 0, \qquad q = h = 0 \quad \text{at } X = m(t). \tag{12}$$

In this study we shall assume that A is a smooth function of its arguments and consider that s is monotone ($s_X \leqslant 0$).

In the special case where the unloaded bed is a horizontal plane and the accumulation-rate does not depend on elevation ($A_s \equiv B_0 \equiv 0$), the stationary-state solution of (8) and (11) can be found in terms of quadratures and is similar to that found for a rigid bed [7,20]

$$h(X) = \zeta_1 \left\{ \int_X^m \left[\int_0^{X_*} A \, \mathrm{d}X^* \right]^{1/n} \mathrm{d}X_* \right\}^{n/(2n+2)}, \tag{13}$$

where $\zeta_1 = \{(2n+2)(n+2)^{1/n}/[n(1-k)]\}^{n/(2n+2)}$. The position of the front of the ice sheet, m, is determined from the condition that the mass flux is zero there

$$\int_0^m A(X) \, \mathrm{d}X = 0. \tag{14}$$

Evidently, the thickness of the ice sheet increases as the bed softness k increases, which is caused by the sinking of the bed.

If the condition of zero mass flux at the front is discarded, then, when $A \equiv \text{const}$, (13) yields

$$h(X) = \zeta_2 \left[1 - \left(\frac{X}{m} \right)^{(n+1)/n} \right]^{n/(2n+2)}, \tag{15}$$

where $\zeta_2 = [2/(1-k)]^{n/(2n+2)}[(n+2)A]^{1/(2n+2)} m^{(n+1)/(2n+2)}$. If we still consider the same form of the bed, but assume that the accumulation rate depends only on elevation, $A_X \equiv B_0 \equiv 0$, $A_s \neq 0$, then a steady-state solution of (8) can be found in inverse form as the function $X(h^{2(n+1)/n})$:

$$X = \zeta_3 \int_f^{f(0)} \left(- \int_0^{f'} A^*(f_*) \, \mathrm{d}f_*/2 \right)^{-1/(n+1)} \mathrm{d}f', \tag{16}$$

where $f = h^{2(n+1)/n}$, $A^*(f) = A(h)$, $\zeta_3 = n(1-k)^{n/(n+1)}/[2(n+1)(n+2)^{1/(n+1)}]$, and $f(0)$ is determined from the equation

$$\int_0^{f(0)} A^* \, \mathrm{d}f_* = 0. \tag{17}$$

In particular, when $n = 3$ and $A = a_1 s^2 - a_2$, where $a_1 > 0$ and $a_2 > 0$ are constants, we can find the solution in the form

$$h = \zeta_4 \left[a_2 - \zeta_5 X^{4/3} \right]^{1/2}, \tag{18}$$

where $\zeta_4 = 7^{1/2}/[2a_1^{1/2}(1-k)]$ and $\zeta_5 = (6a_1/7)^{4/3}(5/2)^{1/3}(1-k)^{5/3}$. For $a_1 = a_2 = 1$ and $k = 0.3$, the solution is depicted in Fig. 2.

It should be noted that, if we consider the above formulas after replacing k by $r < k$, then these solutions describe the case where the unloaded bed elevation is $(k-r)h$, while its softness is still equal to k. Moreover, when the bed is a horizontal plane and the accumulation, A, is zero, then the evolution equation for the ice sheet on an elastic bed (8) can be converted into the usual form describing propagation of a viscous gravity current over a rigid plane by renormalising time by $(1-k)^n$. Therefore, self-similar solutions derived for the latter problem also describe the situation when the bed is elastic after proper renormalisation.

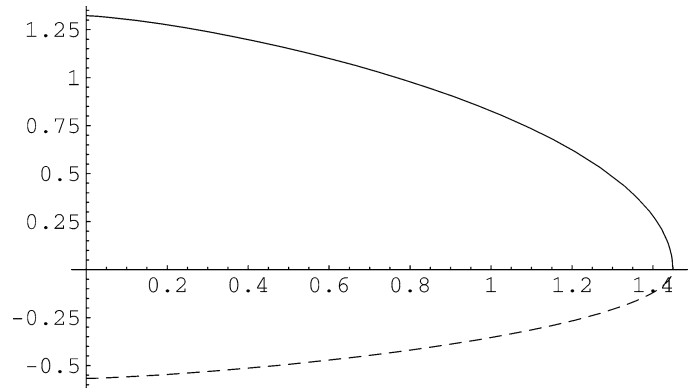

Fig. 2. The steady-state solution (18) with $a_1 = a_2 = 1$ and $k = 0.3$. The solid line is the upper surface, the dashed line is the bed.

3. Analysis of perturbation equations

For the subsequent analysis it is convenient to introduce new variables, in which the whole length of the ice sheet is unity and its front is situated at the origin of the coordinate system, while the divide is at $x = 1$,

$$x = 1 - X/m(t), \quad \tau = t.$$

In the new variables the evolution equation (8) takes the form

$$h_\tau = -(1-x)\frac{m_\tau}{m}h_x + \frac{1}{m}q_x + A\big(s, m(1-x)\big), \quad 0 < x < 1, \tag{19}$$

with the expression for the horizontal mass flux

$$q = \frac{1}{(n+2)m^n}h^{n+2}s_x^n \tag{20}$$

and the boundary conditions are

$$q = h = 0 \quad \text{at } x = 0, \qquad q = 0 \quad \text{at } x = 1. \tag{21}$$

Let us denote by $h_0,\ m_0$ a stationary-state solution of (19). To find a perturbation solution of (19)–(21) about the stationary solution, we use the expansion in terms of the small perturbation amplitude ε and neglect terms of order $O(\varepsilon^2)$

$$\begin{aligned}
&h = h_0 + \varepsilon\,\mathrm{e}^{-\lambda\tau}h_1, \qquad m = m_0 + \varepsilon\,\mathrm{e}^{-\lambda\tau}m_1, \qquad \frac{q}{m} = q_0 + \varepsilon\,\mathrm{e}^{-\lambda\tau}\tilde{q}_1,\\
&B_0\big(m(1-x)\big) = b_0 - \varepsilon\,\mathrm{e}^{-\lambda\tau}b_{0x}m^*(1-x),\\
&s = b_0 + (1-k)h_0 + \varepsilon\,\mathrm{e}^{-\lambda\tau}\big[(1-k)h_1 - b_{0x}m^*(1-x)\big],\\
&A\big(s, m(1-x)\big) = a + \varepsilon\,\mathrm{e}^{-\lambda\tau}\big\{a_s\big[(1-k)h_1 - b_{0x}m^*(1-x)\big] - a_x m^*(1-x)\big\},
\end{aligned} \tag{22}$$

where $a(s_0, x) = A(s_0, m_0(1-x))$, $a_s = A_s(s_0,\ m_0(1-x))$, $b_0(x) = B_0(m_0(1-x))$, $m^* = m_1/m_0$ and $s_0 = b_0 + (1-k)h_0$.

Substituting (21) into (19)–(21), we derive the leading order problem describing a steady-state solution of (8)

$$q_{0x} + a(s_0, x) = 0, \quad 0 < x < 1, \tag{23}$$

$$q_0 = \gamma h_0^{n+2}s_{0x}^n, \tag{24}$$

$$q_0 = h_0 = 0 \quad \text{at } x = 0, \qquad q_0 = 0 \quad \text{at } x = 1, \tag{25}$$

where $\gamma = 1/[(n+2)m_0^{n+1}]$. The first order problem takes the form

$$q_{1x} + \big[(1-k)a_s + \lambda\big]h_1 = m^*\psi, \quad 0 < x < 1, \tag{26}$$

$$h_1 = q_1 = 0 \quad \text{at } x = 0, \qquad q_1 = m^*\varphi \quad \text{at } x = 1, \tag{27}$$

where

$$q_1 \equiv \tilde{q}_1|_{m^*=0} = \frac{h_0^{n+1}s_{0x}^n}{m_0^{n+1}}h_1 + \nu(1-k)h_0^{n+2}s_{0x}^{n-1}h_{1x}, \tag{28}$$

and

$$\psi = \nu\left\{h_0^{n+2}s_{0x}^{n-1}\left[b_{0x}(1-x)\right]_x\right\}_x + (1-x)(a_s b_{0x} + a_x - \lambda h_{0x}) - (n+1)a, \tag{29}$$

$$\varphi = -\nu h_0^{n+2}s_{0x}^{n-1}b_{0x} \tag{30}$$

do not depend on h_1, and $\nu = n\gamma$. The problem (26), (27) is to find a solution of an inhomogeneous second-order differential equation satisfying three boundary conditions. Because generally a second-order differential equation is closed by only two boundary conditions, the third one can only be satisfied for particular values of λ, the eigenvalues. If $m^* \neq 0$, then m^* is a free parameter, and h_1 is proportional to it. In other words, after dividing (26) by m^*, we can derive a problem for the function $\tilde{h}_1 = h_1/m^*$, which does not include the amplitude of the perturbation of the front position, m^*.

Let us denote the accumulation rate at the front of the ice sheet by $a_{(m)} = a(b_0(0), 0)$, and $c = [-2^n m^{n+1}(n+2)a_{(m)}/(1-k)^n]^{1/(2n+2)}$. The stationary-state solution of (23) has the asymptote

$$h_0 = cx^{1/2} + \mathrm{O}\left(x^{\omega}\right), \tag{31}$$

where $\omega = 3/2$ when $a_s \equiv 0$, and $\omega = 1$ otherwise. In Appendix A, it is shown that a solution to the perturbation thickness equation (26) exists. For arbitrary λ, a solution of the thickness perturbation equation can have two different asymptotes as $x \to 0$. These are $h_1 \simeq x^{-3/2}$ or $h_1 \simeq x^{-1/2}$ with coefficients of proportionality determined by the boundary condition at $x = 1$. The same is also true for an asymptotic solution of the homogeneous version of (26). The fact that the solution depends only on one parameter, which is the coefficient of proportionality, is caused by the degeneration of the second-order perturbation differential equation into a first-order equation at $x = 0$. Here we are interested in the solutions with the weaker singularity, $h_1 \simeq x^{-1/2}$. As $x \to 0$, for an arbitrary λ, the solution of the problem (26) can be written as

$$h_1 = \beta_1 x^{-1/2} + \beta_2 + \mathrm{O}\left(x^{1/2}\right) \tag{32}$$

with β_1 determined by the boundary condition at $x = 1$ and the value of λ, and

$$\beta_2 = -\frac{2^n m_0^{n+1}}{c^{2n}(1-k)^n}\left\{\lambda m^* + \frac{2}{c}\left[(1-k)a_s\left(b_0(0),0\right) + \lambda\right]\beta_1\right\}. \tag{33}$$

The solution of the corresponding homogeneous problem, v_1, can be written as

$$v_1 = \alpha(x + \alpha_1) + \mathrm{O}\left(x^{1/2}\right), \tag{34}$$

where α is determined by the boundary condition at $x = 1$, and α_1 is completely determined by the coefficients of Eq. (26). If the boundary condition at $x = 1$ is homogeneous, then α is a free parameter describing the amplitude of the normal mode, and it is non-zero only when λ is an eigenvalue. Because β_1 is determined by the boundary condition at $x = 1$ and the value of λ, its value is generally not zero and the solution is unbounded. Evidently such a behaviour of h_1 contradicts the assumption that $\varepsilon h_1 \ll h_0$, and the expansion (21) is singular. However, if λ is an eigenvalue of the corresponding homogeneous problem with the homogeneous boundary condition at $x = 1$, then the sum $h_1 + v_1$ still satisfies Eq. (26) and the boundary condition at $x = 1$. Moreover, because in this case α is a free parameter, it can be chosen to be equal to $-\beta_1$ to remove the term of order $x^{-1/2}$ and the corresponding bounded solution can be written as

$$h_1 = \beta + \mathrm{O}\left(x^{1/2}\right), \tag{35}$$

where

$$\beta = -m_0^{n+1}2^n m^* \lambda c^{-2n}/(1-k)^n. \tag{36}$$

Therefore, the bounded solution of the problem (26) will satisfy the boundary condition at $x = 1$ if λ is an eigenvalue of the corresponding homogeneous problem, which can be obtained with the assumption $m_1 = 0$.

Although the perturbation is found to be bounded as $x \to 0$, it does not satisfy the boundary conditions at the flow front $(27)_1$. Moreover, it is still much larger than h_0 near the front: $h_1/h_0 \propto x^{-1/2}$. In order to find the cause of the singularity, let us analyse the unsteady solution of (19) near the front. In the vicinity of the front the term q_x is always positive, A is negative, while the first term of the right-hand side of (19) is positive for the retreating front, $m_\tau < 0$, and negative for the advancing front, $m_\tau > 0$. Because $h_\tau = \mathrm{O}(h) \ll h_x$ for small x, there are two asymptotic possibilities for h as $x \to 0$. Firstly, the first two terms at the right-hand side of (19) can balance. This can be true only for the advancing front, and yields

$$h \sim \left[m_\tau(n+2)m^n/(1-k)^n\right]^{1/(2n+1)}x^{n/(2n+1)}. \tag{37}$$

The same asymptotic behaviour is determined by analytical self-similar solutions [21,22]. Secondly, if the first and the third terms are balanced, which determines the retreating front, we have

$$h \sim a_{(m)}(m/m_\tau)x. \tag{38}$$

In the above $m_\tau \simeq \varepsilon$, and the front retreats only due to the mass ablation at the free surface. Evidently, the unsteady solutions have asymptotic behaviour different from that of the stationary solution (31). Therefore, the expansion (21) is only valid outside of the region where $h_0/h \to 0$ as $\varepsilon \to 0$. In both cases describing advancing and retreating of the ice sheet front, $h_0/h \simeq 1$ for $x \simeq \varepsilon^2$, which determines $h \simeq \varepsilon$. These estimates determine the size of the singular layer and the function inside it.

In order to analyse the solution in the singular layer region, we introduce the inner variables $\xi = x/\varepsilon^2,\ H = h/\varepsilon,\ m = m_0 + \varepsilon M_1(\tau)$. The problem (19) takes the form

$$-\frac{M_{1\tau}}{m_0} H_\xi + \nu(1-k)^n \left(H^{n+2} H_\xi^n\right)_\xi + a_{(m)} = \mathrm{O}(\varepsilon), \tag{39}$$

$$H = H^{n+2} H_\xi^n = 0 \quad \text{at } \xi = 0. \tag{40}$$

As $\xi \to \infty$, the solution of the above problem can be found to be

$$h = \varepsilon H = \varepsilon\left(c\xi^{1/2} + \chi\right) + \varepsilon \mathrm{O}\left(\xi^{-1/2}\right) + \mathrm{O}\left(\varepsilon^2\right), \tag{41}$$

where $\chi = 2^n c^{-2n} m_0^n M_{1\tau}/(1-k)^n$. In the vicinity of the front, the outer solution for h, given by the expansion (21), can be written as

$$h = cx^{1/2} + \varepsilon\, \mathrm{e}^{-\lambda\tau}\beta + \mathrm{O}(x) + \mathrm{O}\left(\varepsilon x^{1/2}\right) + \mathrm{O}\left(\varepsilon^2\right), \quad x \to 0. \tag{42}$$

Matching requires $M_{1\tau} = -\lambda m_1$, which is satisfied for $M_1 = \mathrm{e}^{-\lambda\tau} m_1$.

To summarise, we have shown that the linear stability of a stationary ice sheet converts to the problem of the linear stability of the ice sheet with fixed position of its front, described by the singular homogeneous equation (26). The singularity of the expansion is caused by different asymptotic behaviours of the stationary-state solution and non-stationary one, and can be treated by the method of matched asymptotic expansions, while the eigenvalues can be found by considering the outer solution only with eigenvalues determined by the homogeneous eigenvalue problem. In many works (e.g., [8]), the ice sheet front is assumed to be fixed in time; in Appendix B we treat the singularity of the perturbation expansion with fixed front.

4. Sensitivity of ice sheet stability to bed conditions and equilibrium line

Here we consider numerical solutions of (23)–(25) which determine the stationary problem, and the homogeneous perturbation problem (26). In developing numerical approximations of (23) and (26) the singularities at the front of the ice sheet, $h_{0x} = \mathrm{O}(x^{-1/2}),\ h_1 = \mathrm{O}(x^{-1/2})$, were removed by introduction of the new independent variable and smooth functions $y = x^{1/2},\ \tilde{h}_1 = h_1 y,\ \tilde{h}_0 = h_0/y$. Tests showed convergence of the numerical schemes.

We focus on the influence of the bed softness, bed slope and equilibrium line inclination on the stability of the ice sheet, and consider the simple linear functions

$$B|_{t=0} = b_1 X, \tag{43}$$

$$A = a_1 s + a_2 + a_3 X, \tag{44}$$

where $b_1,\ a_1,\ a_2,\ a_3$ are constants. Parameters $b_1,\ a_1,\ -a_3/a_1$ represent the bed slope, vertical gradient of the mass balance with respect to altitude, and equilibrium line inclination (line at which $A = 0$) respectively. The equilibrium line altitude is given by the formula $z = -(a_2 + a_3 X)/a_1$, and $-a_2/a_1$ is the equilibrium line altitude at the divide. In order to determine the influence of the bed softness on the stability of the ice sheet, we will assume that the initial bed elevation $B|_{t=0}$, found for $k = 0$, is also valid for different values of its softness k and the same values of the other parameters. Such an assumption preserves the geometry of the ice sheet for different k and corresponds to the existence of an initial bump on the bed with the thickness kh. We set the flow-law exponent $n = 3$ and the maximum value of $k = 0.3$ as typically adopted in modelling ice sheet dynamics [14,19].

In the numerical experiments, the minimum eigenvalue λ as a function of the bed slope b_1 and equilibrium line inclination a_3 is found, while the other parameters are fixed. The numerical experiments showed that in many cases there exist two solutions of the leading-order problem (23) with different positions of the front of the stationary ice sheet, m_0.

In Figs. 3 and 4, we show results of computations when the equilibrium line is situated higher than the bed, $a_2 < 0$. In this case although non-trivial stationary-state solutions can exist, natural formation of the ice sheet due to the mass accumulation is impossible, and it is assumed that it originally formed under different accumulation conditions. The dependence of λ on the bed slope, b_1, is presented in Fig. 3. Positive values of λ show stable solutions and negative values show unstable solutions. The left (right) half of the coordinate plane $b_1 < 0$ ($b_1 > 0$) corresponds to a negative (positive) downstream bed slope. Nine curves are shown: the solid lines correspond to $k = 0$, dashed to $k = 0.15$ and dotted-dashed to $k = 0.3$; the three curves for each value of

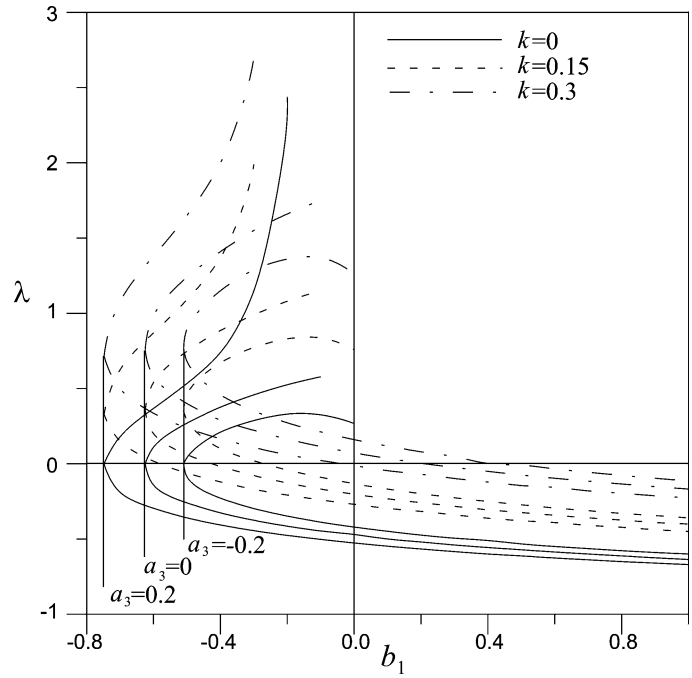

Fig. 3. The dependence of the minimum eigenvalue, λ, on the bed slope, b_1, when the equilibrium line is higher than the bed, $a_2 < 0$. When b_1 increases, the length of the ice sheet, m_0, decreases at the lower branch and increases at the upper branch increases. The rate of the increase is higher than the rate of the decrease.

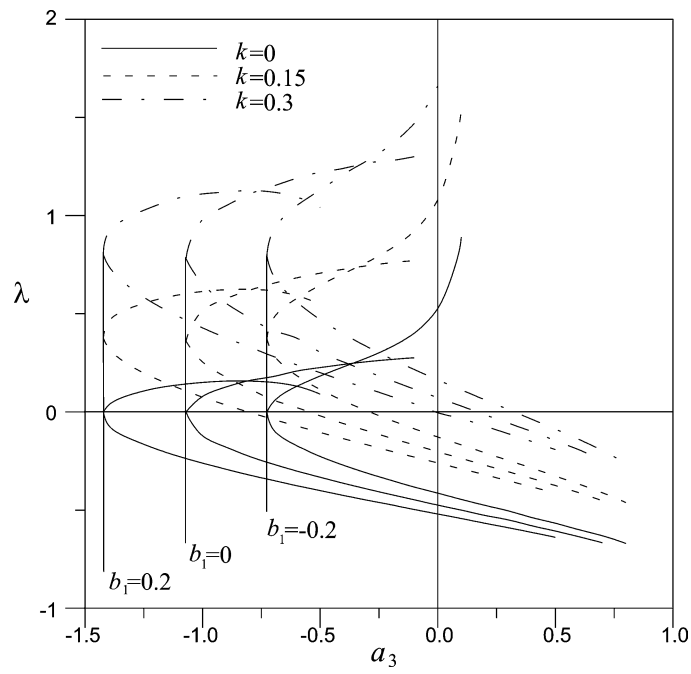

Fig. 4. The dependence of the minimum eigenvalue, λ, on the equilibrium line inclination, a_3, when the equilibrium line is higher than the bed, $a_2 < 0$. When a_3 increases, the length of the ice sheet, m_0, decreases at the lower branch and increases at the upper branch. The rate of the increase is higher than the rate of the decrease.

k are determined by $a_3 = 0.2,\ a_3 = 0,\ a_3 = -0.2$, which correspond to negative, zero and positive equilibrium line inclination respectively ($a_1 = 1,\ a_2 = -0.5$ are fixed). All the curves have lower and upper branches, corresponding to two stationary-state solutions. With increasing bed slope b_1, the length of the ice sheet, m_0, increases at the upper branch and decreases at the lower branch. A stationary-solution at the upper branch describes a longer ice sheet than the lower branch. Moreover, as computations showed, the rate of the increase of m_0 with b_1 at the upper branch is much higher than the rate of its decrease at the lower branch. When the bed is rigid, $k = 0$, and its slope is negative, $b_1 < 0$, the longer and shorter stationary-state solutions are stable and unstable, respectively. These solutions merge at the axis $\lambda = 0$ determining neutral equilibrium. The computations showed that for the stationary-state solutions on the upper branch, the length of the ice sheet $m_0 \to +\infty$ as $(b_1 + a_3/a_1) \to -0$. This is because in order to sustain zero mass-balance of the stationary ice sheet, the length of the ice sheet must increase as the angle between the flat bed and straight equilibrium line decreases, thereby maintaining a sufficiently large region of ablation. Moreover, this is possible only if the bed and the equilibrium line do not cross, $b_1 \leqslant -a_3/a_1$.

The dependence of λ on the equilibrium line inclination represented by a_3 is depicted in Fig. 4. The left (right) half of the coordinate plane $a_3 < 0$ ($a_3 > 0$) corresponds to positive (negative) downstream equilibrium line inclination. Again, nine curves are shown: the solid lines correspond to $k = 0$, dashed to $k = 0.15$ and dotted-dashed to $k = 0.3$; the three curves for each value of k are determined by $b_1 = 0.2,\ b_1 = 0$, and $b_1 = -0.2$, which corresponds to positive, zero and negative bed slope respectively ($a_1 = 1,\ a_2 = -0.5$ are fixed).

With increasing a_3, the length of the stationary ice sheet m_0 increases on the upper branch and decreases on the lower branch, and the rate of increase at the upper branch is much higher than the rate of decrease at the lower branch. The situation is similar to that depicted in Fig. 3, which also concerns the limiting values $(a_3 + b_1 a_1) \to -0$.

Figs. 5 and 6 show results of the computations for the dependence of λ on bed slope b_1 and equilibrium line inclination represented by a_3, respectively, when the equilibrium line is not higher than the highest point of the bed ($a_2 \leqslant 0$). All values of the parameters of the problem are the same as before, except $a_2 = 0.5$ instead of $a_2 = -0.5$. In this case there are no unstable branches because as the equilibrium line approaches the bed at the divide, $a_2 \to -0$, the length of the unstable ice sheet tends to zero, and the values of b_1 and a_3, determining neutral equilibrium, tend to $-\infty$. It should be noted that for the stable solutions, the gradient of λ is positive when $a_2 = -0.5$ and negative when $a_2 = 0.5$, except the regions where $(a_3 + b_1 a_1) \to -0$, namely near the right ends of the branches.

From Figs. 3–6 it can be seen that increasing the softness of the bed, k, has a stabilising effect on the ice sheet. Moreover, for the chosen range of values of k, the dependence of λ on k is close to linear.

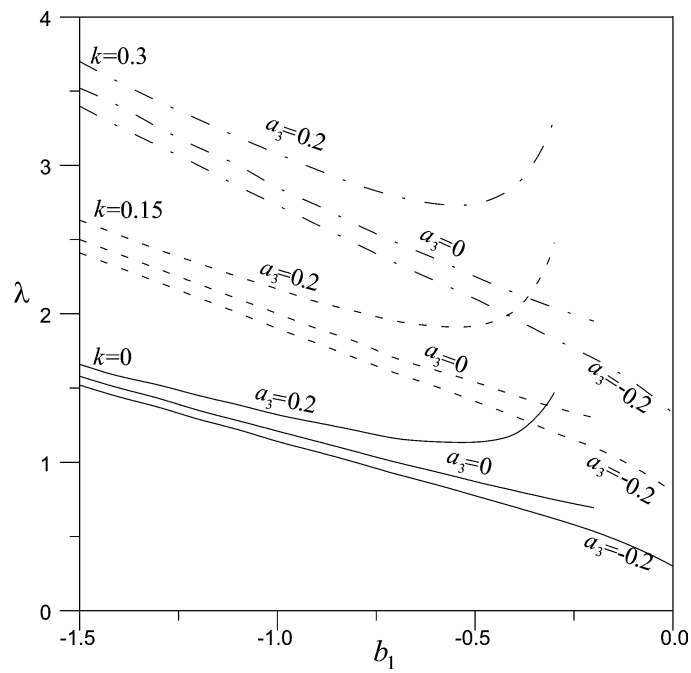

Fig. 5. The dependence of the minimum eigenvalue, λ, on the bed slope, b_1, when the equilibrium line is lower than the bed, $a_2 > 0$.

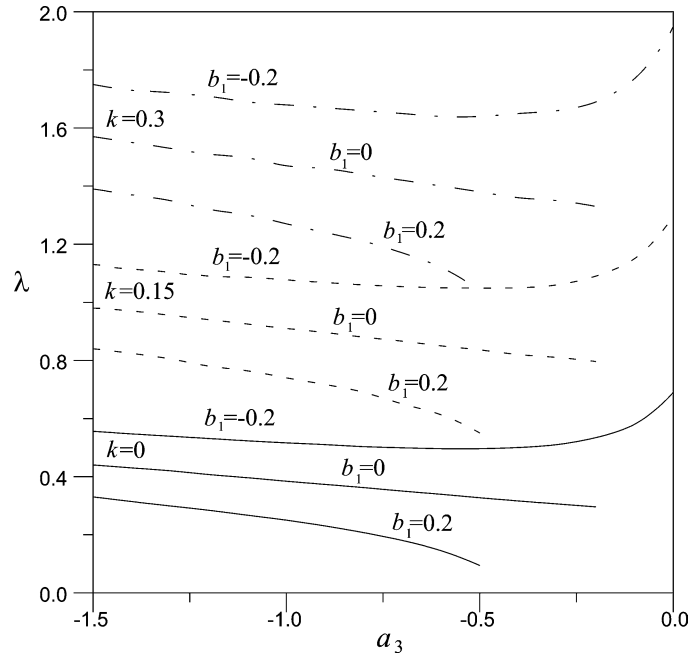

Fig. 6. The dependence of the minimum eigenvalue, λ, on the equilibrium line inclination, a_3, when the equilibrium line is lower than the bed, $a_2 > 0$.

We now show that if the bed and equilibrium line are horizontal lines, $b_1 \equiv a_3 \equiv 0$, then a change of the gradient of accumulation with altitude a_1 and a_2 do not affect the stability. Let $\hat{h}$ be a solution of the equations

$$\hat{h}_{\hat{\tau}} + \big(\hat{h}^{n+2}|\hat{s}_{\widehat{X}}|^n\big)_{\widehat{X}}/(n+2) = \hat{A}\big(\hat{s}, \widehat{X}\big), \quad \hat{s} = \widehat{B}|_{\hat{\tau}=0} + \hat{h} - k\big(\hat{h} - \hat{h}|_{\hat{\tau}=0}\big), \tag{45}$$

where

$$\begin{aligned} &\widehat{B}|_{\hat{\tau}=0}\big(\widehat{X}\big) = B|_{\tau=0}\big(X_*\widehat{X}\big)/h_*, \qquad \hat{A}\big(\hat{s}, \widehat{X}\big) = A\big(h_*\hat{s}, X_*\widehat{X}\big)X_*^{n+1}/h_*^{2n+2}, \\ &\widehat{X} = X/X_*, \qquad \hat{h} = h/h_*, \qquad \hat{\tau} = \tau h_*^{2n+1}/X_*^{n+1}, \end{aligned} \tag{46}$$

and $X_*,\ h_* = \text{const}$. Eqs. (45) are found by rescaling of (8) and (11). If $h(\tau, X)$ is a solution of (8), then

$$\hat{h}(\hat{\tau}, \widehat{X}) = h\big(X_*^{n+1}\hat{\tau}/h_*^{2n+1}, X_*\widehat{X}\big)/h_*$$

is a solution of (45). For the case considered, we have $\widehat{B}|_{\hat{\tau}=0}(\widehat{X}) = \hat{b}_1\widehat{X}$, where $\hat{b}_1 = b_1X_*/h_*$, and $\hat{A} = \hat{a}_1\hat{s} + \hat{a}_2 + \hat{a}_3\widehat{X}$ with

$$\hat{a}_1 = a_1X_*^{n+1}/h_*^{2n+1}, \quad \hat{a}_2 = a_2X_*^{n+1}/h_*^{2n+2}, \quad \hat{a}_3 = a_3X_*^{n+2}/h_*^{2n+2}.$$

If $b_1 \equiv a_3 \equiv 0,\ a_1 > 0,\ a_2 < 0$ and h is the solution found for particular values $a_1 = \tilde{a}_1,\ a_2 = \tilde{a}_2$, then for any values a_1, a_2 equating $\hat{a}_1 = \tilde{a}_1,\ \hat{a}_2 = \tilde{a}_2$ gives us two equations for the determination of $h_*,\ X_*$, which determines $\hat{h}(\widehat{X}, \hat{\tau}) = h(\widehat{X}, \hat{\tau})$. Therefore, in variables $\hat{h},\ \widehat{X},\ \hat{\tau}$ we have the same solutions and the same eigenvalues for any $a_1 > 0,\ a_2 < 0$.

Experiments showed stability of the ice sheet when $a_2 = 0.5,\ a_3 = -1$ and $a_1 = 0$ (the accumulation rate does not depend on elevation) and bed slope b_1 is arbitrary (solution $h(X, \tau, b_1)$). In this case equating $\hat{a}_2 = 0.5,\ \hat{a}_3 = -1$ for any $a_2 > 0,\ a_3 < 0$ allows us to find $X_*,\ h_*$ and $\hat{b}_1 = b_1X_*/h_*$, such that $\hat{h}(\widehat{X}, \hat{\tau}) = h(\widehat{X}, \hat{\tau}, \hat{b}_1)$. Therefore, the ice sheets are stable when $a_1 = 0$ for arbitrary $a_2 > 0,\ a_3 < 0,\ b_1$.

Evidently, if the equilibrium line touches the bed at the divide, $a_2 \equiv 0$, and we have a flat horizontal bed $b_1 \equiv 0$ (and the equilibrium line inclination, a_3, can change) or $a_3 \equiv 0$ (and b_1 can change), with fixed vertical gradient of the accumulation a_1, then all solutions of this problem will be similar and determine the same eigenvalue.

5. Discussion of results

We have shown that the linear stability analysis for the stationary ice sheet with perturbed position of its front converts to that describing the ice sheet with fixed front. Therefore, for interpretation of the numerical experiments we consider the homogeneous form of the perturbation problem (26). Integrating along the length of the ice sheet, we have

$$q_1|_{x=0} - \int_0^1 (1-k)a_s h_1 \,\mathrm{d}x = \lambda \int_0^1 h_1 \,\mathrm{d}x. \tag{47}$$

This equation shows us that if the mass flux at the front, q_1, caused by the perturbation, is larger than the additional accumulation rate due to the changed surface elevation (the second term in (27)), the stationary-state solution is stable, and vice versa.

The more negative the bed slope is, the stronger will be the influence of the gravity force acting along the direction of the flow. For two ice sheets of the same length but different thicknesses flowing over the same bed, the influence of the bed slope will be stronger on the ice sheet with smaller thickness; it can be negligible for an ice sheet with thickness much larger than the typical change of the bed elevation. The larger the negative bed slope in comparison with the thickness gradient, the stronger will be influence of the gravity force on the ice flow. This leads to a larger perturbed mass flux at the front q_1 and is stabilising.

The flow of the ice is influenced by the kinematic boundary condition at the upper surface of the ice sheet. An increase of the equlibrium line inclination corresponds to an increase of the longitudinal gradient of the mass accumulation. In the accumulation zone upstream, the ice sheet surface is almost horizontal and the accumulation increase on a positive perturbation is determined mainly by its vertical gradient, A_s, which does not change when the equilibrium line inclination increases. In the zone of ablation downstream, however, the upper surface is steep, and the ablation change on the surface perturbation is determined mainly by the longitudinal accumulation gradient. Thus, an increase in equilibrium line inclination diminishes the cumulative effect of accumulation increase, and has a stabilising effect. As in the case of the influence of the bed slope, the equilibrium line inclination effects longer ice sheets (with smaller aspect ratio) greater than shorter ones (larger aspect ratio). This is because an incremental change in equilibrium line inclination changes the areas of ablation and accumulation more greatly for long ice sheets than for short ice sheets.

These two effects can be illustrated if we assume that the front of the ice sheet moves. In this case, instability means unrestricted advance or retreat of the front. When the bed slope is negative, a positive perturbation of the surface will lead to advancing and lowering of the front, which will be counteracted by increased ablation at it. The existence of such a counteracting mechanism will lead to stabilisation of the ice sheet. A similar situation will occur if we consider existence of a horizontal gradient of the accumulation rate. If the gradient is negative, then advancing of the front will again lead to an increase of ablation at it, which has a stabilising effect on the motion. The strength of these effects depends also on the length of the ice sheet and its aspect ratio.

In Figs. 3 and 4, there are two perturbation solutions (stable and unstable) for the same data set and the stable ice sheet is longer then the unstable one. The longer the ice sheet is, the smaller is its average thickness gradient (6) and the greater is the influence of bed slope. The experiments (Fig. 3) show that small changes of the bed slope lead to large changes of the length of the stable ice sheets. Therefore, a small increase of a negative value of the bed slope causes a large decrease of the length of the ice sheet leading to a reduced dependence of the flow on the bed slope and a decrease of the minimum (stable) eigenvalue, which is destabilising. When the ice sheet is unstable, an increase of the negative bed slope leads to an increase in length of the ice sheet and λ (stabilising).

As the horizontal equilibrium line becomes lower and reaches the bed, changes of the bed slope and the length of the ice sheet attain a self-consistent regime with similarity of the solutions, and changes in the bed slope do not effect the stability. However, when the equilibrium line lowers beneath the bed, $a_2 > 0$, the change of the length of the ice sheet is not large enough relative to a change of the bed slope, which is destabilising, Fig. 5. Similar results can be derived for the influence of the equilibrium line inclination (Figs. 4, 6).

An interesting behaviour can be seen near the right ends of the stable branches (Figs. 3 and 4) when the bed slope or the equilibrium line inclination tend to their limiting values, $(a_3 + b_1 a_1) \to -0$, and become parallel. For $a_1 = 1$, in this case the absolute values of a_3 and b_1 become close to each other, but have different signs. Therefore, the effects of the bed slope and equilibrium line inclination counteract. However, as the computations show, the bed slope has a stronger influence on the flow stability, which yields the corresponding stabilising or destabilising of the ice sheet, which depends on the bed slope under consideration: the positive bed slope leads to destabilisation; negative bed slope leads to stabilisation.

When the bed is non-rigid, and its dynamics is described by the law of elasticity or hydrostatic equilibrium, the perturbation of the upper surface will lead to instant sinking of the bed, and diminishing of the surface rise caused by the perturbation, which is accounted for by the factor $1-k$ at the second term in (47), describing an increase of the accumulation rate due to the surface perturbation. This process has a stabilising effect on the ice sheet motion, which is also confirmed by the computations.

6. Concluding remarks

The linear stability of an ice sheet with a power-law rheology on an elastic layer under the action of elevation-dependent surface mass-accumulation is determined by the bed slope, equilibrium line position and bed softness (elastic modulus of the elastic layer). For the considered linear form of the bed profile and the equilibrium line, we conclude that if the equilibrium line is situated higher than the bed, preventing natural formation of the ice sheet under the present conditions, there exists two solutions, stable and unstable if the equilibrium line inclination is larger than the bed slope, and only an unstable solution otherwise. An increase of the negative bed slope or positive equilibrium line inclination leads in this case to stabilisation of the unstable solution (increasing of the eigenvalues) and destabilisation of the stable ones (decreasing of the eigenvalues) with coincidence at neutral equilibrium. When the position of the equilibrium line becomes closer to the bed, the length of the unstable ice sheet tends to zero, and when it touches the bed at the divide, there are no unstable solutions. If the bed slope or equilibrium line inclination is zero, all solutions are similar, and a change of either bed slope or equilibrium line inclination (whichever is non-zero) does not change the eigenvalues, and does not affect stability.

If the equilibrium line is situated lower than the bed, which is the case of natural formation of the ice sheet, then there exist only stable solutions. In this case, an increase of the negative bed slope or positive equilibrium line inclination leads to stabilisation of the stable solutions.

An increase of the softness of the bed (decrease of its elastic modulus) has a stabilising effect on the ice sheet, due to its sinking under the additional load caused by the surface perturbation.

When the ice sheet is unstable, we suggest that a two-dimensional perturbation of the ice sheet surface can lead to advancing of the parts with positive perturbation and retreating of those with negative ones, leading to fingering of the flow front.

Appendix A. Existence of perturbation solution

Here, we ascertain that the solution of (26) exists. Because the boundary condition at $x = 1$ can be converted into homogeneous form by the substitution $v = h_1 - h^*$, where h^* is a smooth function satisfying the condition at $x = 1$, we can write the problem (26) in an operator form

$$Dv = f, \quad v \in \Omega, \tag{A.1}$$

where $\Omega := \{v \in C^2(0,1]:\ v_x(1) = 0;\ v < \infty,\ x \to 0\}$. The Fredholm alternative, [23], determines the condition of the existence of a solution of (A.1):

$$\langle f, v^* \rangle = 0, \tag{A.2}$$

where $\langle \cdot, \cdot \rangle$ is a scalar product, and v^* is a solution of the homogeneous conjunctive problem

$$D^* v^* = 0, \quad v^* \in \Omega. \tag{A.3}$$

However, because the operator under consideration D^* determines only unbounded non-trivial solutions of the homogeneous equation (A.3) at $x = 0$, the only bounded solution of the homogeneous problem (A.3) is the trivial one, $v \equiv 0$, and (A.2) is satisfied for arbitrary f. This was not recognised in [12], and the condition (A.2) was considered to be a strong restriction on the existence of the solution searched for as a normal mode, while accounting for the front dynamics.

Appendix B. Singularity of the perturbation at the fixed front

In Section 3, it was shown that if the front of the ice sheet moves during the perturbation, the outer and inner solutions can be matched only if the outer is bounded. However, the stability analysis converts to that describing the linear stability of the ice sheet with fixed position of its front which yields a homogeneous perturbation problem with unbounded outer solution, [7,8]. Since the stationary-front perturbation solutions have been frequently used with zero ice thickness at the front, [8,9,24], here we ascertain that the unbounded solution of the singular homogeneous eigenvalue problem (26) can be matched with the inner solution near the front to give a bounded solution.

For simplicity, we consider the case when the bed is a horizontal plane and the accumulation rate does not depend on elevation, $b_0 \equiv a_s \equiv 0$. Consider the behaviour of the solution of (8) as $x \to 0$ when the horizontal mass flux at the front (denoted here by $-q_{(m)}m$, where $q_{(m)} = q|_{x=0}/m$) is non-zero,

$$h \sim \frac{c}{\sqrt{-a_{(m)}}} \left\{ (q_{(m)} - a_{(m)}x)^{(n+1)/n} - q_{(m)}^{(n+1)/n} \right\}^{n/(2n+2)}. \tag{B.1}$$

Evidently, when $-a_{(m)}x \ll q_{(m)}$, we have $h \simeq x^{n/(2n+2)}$, while, when $q_{(m)} \ll -a_{(m)}x$, the asymptote coincides with that found for h_0 (31). This means that the functions h and h_0 have different asymptotic behaviour as $x \to 0$. In order to find the thickness of the boundary layer near the front, where expansion (21) is not valid, we integrate (19) with respect to x from 0 to 1 to obtain

$$q^{(m)} = -\int_0^1 h_\tau \,\mathrm{d}x = \mathrm{O}(\varepsilon). \tag{B.2}$$

As $\varepsilon \to 0$, the leading-order term h_0 does not approximate the solution h when $q_{(m)} \simeq -a_{(m)}x$, namely when $x \simeq \varepsilon$. The same result can be obtained from comparison of the leading and first-order solutions: $h_0 \simeq \varepsilon h_1 \simeq \varepsilon^{1/2}$, when $x \simeq \varepsilon$. Therefore, expansion (21) with $m^* = 0$ breaks down when $x \simeq \varepsilon$.

To find the inner solution in the vicinity of the front, we introduce the inner variable and function $\xi = x/\varepsilon,\ H = h/\varepsilon^{1/2}$. In these new variables the evolution equation takes the form

$$\begin{aligned} &\varepsilon^{1/2} H_\tau = \nu(1-k)^n \left(H^{n+2} H_\xi^n\right)_\xi + a_{(m)} + \mathrm{O}(\varepsilon), \quad \xi > 0, \\ &H = 0 \quad \text{at } \xi = 0. \end{aligned} \tag{B.3}$$

Expanding $H = H_0 + \mathrm{O}(\varepsilon^{1/2})$, we derive the leading order term

$$H_0 = \frac{c}{\sqrt{-a_{(m)}}} \left\{ [Q - a_{(m)}\xi]^{(n+1)/n} - Q^{(n+1)/n} \right\}^{n/(2n+2)}, \tag{B.4}$$

where Q is a parameter to be determined from a matching procedure.

The inner solution is

$$h = H\varepsilon^{1/2} = \varepsilon^{1/2}\left[c\xi^{1/2} - \frac{c}{2a_{(m)}} Q\xi^{-1/2} \right] + \varepsilon^{1/2}\left(\xi^{-(n+2)/(2n)}\right) + \mathrm{O}(\varepsilon), \quad \xi \to \infty. \tag{B.5}$$

The outer solution is

$$h = cx^{1/2} + \varepsilon\, \mathrm{e}^{-\lambda\tau}\left[\alpha x^{-1/2} + \mathrm{O}(1)\right] + \mathrm{O}\left(x^{3/2}\right) + \mathrm{O}\left(\varepsilon^2\right), \quad x \to 0. \tag{B.6}$$

Matching requires $Q = -2a_{(m)}\alpha\, \mathrm{e}^{-\lambda\tau}/c$.

Hence, in the case of a stationary ice front, the singularity arising in the expansion of the thickness of the ice sheet about the stationary-state solution can be treated using matched asymptotic expansions and does not affect the eigenvalues λ.

References

[1] H.E. Huppert, The propagation of two-dimensional and axisymmetric viscous gravity currents over a rigid horizontal surface, J. Fluid Mech. 121 (1982) 43–58.
[2] H.E. Huppert, The intrusion of fluid mechanics into geology, J. Fluid Mech. 173 (1986) 557–594.
[3] J.E. Simpson, Gravity currents in the laboratory, atmosphere and ocean, Ann. Rev. Fluid Mech. 14 (1982) 213–234.
[4] R.C. Kerr, J.R. Lister, The spread of subducted lithosphere material along mid-mantle boundary, Earth Planet Sci. Lett. 85 (1987) 241–247.
[5] K. Hutter, Theoretical Glaciology, Reidel, Dordrecht, 1983.
[6] D.P. Hoult, Oil spreading in the sea, Ann. Rev. Fluid Mech. 4 (1972) 341–368.
[7] J.F. Nye, The motion of ice sheets and glaciers, J. Glaciol. 3 (26) (1959) 493–507.
[8] A.C. Fowler, Modelling ice sheet dynamics, Geophys. Astrophys. Fluid Dyn. 63 (1992) 29–65.
[9] R.C.A. Hindmarsh, Normal modes of an ice sheet, J. Fluid Mech. 335 (1997) 393–413.
[10] J. Weertman, Stability of ice-age ice sheets, J. Geophys. Res. 66 (1961) 3783–3792.
[11] J. Oerlemans, Modelling the response of valley glaciers to climatic change, in: C. Boutron (Ed.), Physics and Chemistry of the Atmospheres of the Earth and Other Objects of the Solar System, ERCA, vol. II, 1996, pp. 91–123.
[12] A.V. Wilchinsky, Studying ice sheet stability using the method of separation of variables, Geophys. Astrophys. Fluid Dyn. 94 (1–2) (2001) 15–45.
[13] R. Greve, Glacial isostasy: Models for the response of the Earth to varying ice loads, in: B. Straughan, R. Greve, H. Ehrentraut, Y. Wang (Eds.), Continuum Mechanics and Applications in Geophysics and the Environment, Springer, 2001, pp. 307–325.
[14] J.W. Glen, The creep of polycrystalline ice, Proc. R. Soc. London Ser. A 228 (1955) 519–538.
[15] L.D. Landau, E.M. Lifshiz, Theory of Elasticity, Pergamon Press, Oxford, 1986.
[16] A.C. Fowler, D.A. Larson, On the flow of polythermal glaciers I: model and preliminary analysis, Proc. R. Soc. London Ser. A 363 (1978) 217–242.
[17] L.W. Morland, I.R. Johnson, Steady motion of ice sheets, J. Glaciol. 28 (1980) 229–246.

[18] A.N. Salamatin, A.B. Mazo, Similarity analysis of the general mathematical model of an ice-cap glacier, J. Sov. Math. 44 (5) (1984) 664–672.
[19] R. Greve, A continuum-mechanical formulation for shallow polythermal ice sheets, Philos. Trans. R. Soc. London Ser. A 355 (1997) 921–974.
[20] S.S. Vialov, Regularities of ice deformation, in: Physics of the Movement of Ice, International Association of Scientific Hydrology Symposium at Chamonix, 1958, pp. 383–391, publ. 47.
[21] V.A. Chugunov, Group properties of the equation describing glacier flow, Izv. Vyssh. Uchebn. Zaved. Mat. 10 (1982) 84–87.
[22] J. Gratton, F. Minotti, Theory of creeping gravity currents of a non-Newtonian liquid, Phys. Rev. E 60 (6) (1999) 6960–6967.
[23] E. Zeidler, Applied Functional Analysis, in: Appl. Math. Sci., vol. 109, Springer-Verlag, New York, 1995.
[24] J. Gratton, M. Minotti, Self-similar gravity currents: phase-plane formalism, J. Fluid Mech. 210 (1990) 155–182.